Int. J. Radiation Oncology Biol. Phys., Vol. 76, No. 5, pp. 1520–1527, 2010

0360-3016/10/$–see front matter

ELSEVIER

doi:10.1016/j.ijrobp.2009.10.047

BIOLOGY CONTRIBUTION

ACTIVATED MACROPHAGES AS A NOVEL DETERMINANT OF TUMOR CELL RADIORESPONSE: THE ROLE OF NITRIC OXIDE–MEDIATED INHIBITION OF CELLULAR RESPIRATION AND OXYGEN SPARING

Heng Jiang, M.S.,* Mark De Ridder, M.D., Ph.D.,*† Valeri N. Verovski, Ph.D.,† Pierre Sonveaux, Ph.D.,‡ Bénédicte F. Jordan, Ph.D.,§ Kalun Law, B.S.,* Christinne Monsaert, B.S.,* Dirk L. Van den Berge, M.D.,† Dirk Verellen, Ph.D.,† Olivier Feron, Ph.D.,‡ Bernard Gallez, Ph.D.,§ and Guy A. Storme, M.D., Ph.D.*†

*Vrije Universiteit Brussel, Cancer Research Unit, †UZ Brussel, Oncologisch Centrum, Radiotherapie, ‡Unit of Pharmacology and Therapeutics and §Unit of Biomedical Magnetic Resonance, Université catholique de Louvain, Brussels, Belgium

Purpose: Nitric oxide (NO), synthesized by the inducible nitric oxide synthase (iNOS), is known to inhibit metabolic oxygen consumption because of interference with mitochondrial respiratory activity. This study examined whether activation of iNOS (a) directly in tumor cells or (b) in bystander macrophages may improve radioresponse through sparing of oxygen.

Methods and Materials: EMT-6 tumor cells and RAW 264.7 macrophages were exposed to bacterial lipopolysaccharide plus interferon-γ, and examined for iNOS expression by reverse transcription polymerase chain reaction, Western blotting and enzymatic activity. Tumor cells alone, or combined with macrophages were subjected to metabolic hypoxia and analyzed for radiosensitivity by clonogenic assay, and for oxygen consumption by electron paramagnetic resonance and a Clark-type electrode.

Results: Both tumor cells and macrophages displayed a coherent picture of iNOS induction at transcriptional/translational levels and NO/nitrite production, whereas macrophages showed also co-induction of the inducible heme oxygenase-1, which is associated with carbon monoxide (CO) and bilirubin production. Activation of iNOS in tumor cells resulted in a profound oxygen sparing and a 2.3-fold radiosensitization. Bystander NO-producing, but not CO-producing, macrophages were able to block oxygen consumption by 1.9-fold and to radiosensitize tumor cells by 2.2-fold. Both effects could be neutralized by aminoguanidine, a metabolic iNOS inhibitor. An improved radioresponse was clearly observed at macrophages to tumor cells ratios ranging between 1:16 to 1:1.

Conclusions: Our study is the first, as far as we are aware, to provide evidence that iNOS may induce radiosensitization through oxygen sparing, and illuminates NO-producing macrophages as a novel determinant of tumor cell radioresponse within the hypoxic tumor microenvironment. © 2010 Elsevier Inc.

Macrophages, Hypoxia, Oxygen sparing, Radiosensitization, Inducible nitric oxide synthase.

INTRODUCTION

Hypoxia is a common feature of solid tumors, which have median oxygen levels around 1% and frequent regions of deep hypoxia (0.1–1%), contrasting to well-oxygenated normal tissues (1). The lack of oxygen prevents irradiation-induced DNA damage, which may account for up to three times less radiosensitivity compared with aerobic cells. Clearly, this impaired tumor radioresponse reflects the imbalance between oxygen supply and metabolic oxygen depletion (MOD). Computer simulations linked to experimentally derived data predicted that pharmacologically forced inhibition of MOD may be significantly more efficient to abolish tumor hypoxia, as compared with increased blood perfusion (2). In line, some glucocorticoids, known to inhibit oxidative phosphorylation in the mitochondrial respiratory chain, enhanced oxygenation and radiosensitivity in a mouse tumor model despite decreased tumor perfusion (3).

In this context, we have focused efforts to revisit MOD with special regard to nitric oxide (NO), which is synthesized from *L*-arginine by a family of nitric oxide synthases (NOS) and is involved in neurotransmission, vasodilation, immunoreactivity, and mitochondrial oxygen homeostasis (4, 5). Our

Reprint requests to: Mark De Ridder, UZ Brussel, Oncologisch Centrum, Radiotherapie, Laarbeeklaan 101, B-1090 Brussels, Belgium. Tel: (+32) 2-477-6147; Fax: (+32) 2-477-6212; E-mail: mark.deridder@uzbrussel.be

Supported by The Foundation Against Cancer, Foundation of Public Interest (Grant (219.2008), Fonds voor Wetenschappelijk Onderzoek–Vlaanderen (Grant 0386-07), Onderzoeksraad van de Vrije Universiteit Brussel, and Scientific Fund W. Gepts UZ-Brussel.

Conflict of interest: none.

Acknowledgment—The authors thank Dr. M. Mareel for critical reading and reviewing of the manuscript.

Received July 17, 2009, and in revised form Oct 9, 2009. Accepted for publication Oct 14, 2009.

concept is to block MOD aiming at oxygen sparing above 1%, where little if any loss of radiosensitivity occurs. We previously reported that tumor radioresponse may be affected through the endothelial isoform of nitric oxide synthase (eNOS), an enzyme that controls vasodilation. Indeed, the eNOS inducer insulin was able to increase both tumor oxygenation and radioresponse in a liver TLT and fibrosarcoma FSAII mouse tumors through the inhibition of MOD (6, 7). Consistently, the eNOS inhibitor L-NAME counteracted the effects of insulin, hence resembling the lack of radiosensitization in eNOS knockout mice. This approach showed more radiation-induced regrowth delays than carbogen treatment and therefore illuminated NO as an intrinsic radiosensitizer next to its oxygenation signature.

This intrinsic radiosensitizing ability of NO has been ultimately dissected and described in tumor cells that overexpress iNOS, a cytokine-inducible isoform, whose activation efficiently reversed hypoxic radioresistance by generating high levels of NO (8). Identified first in activated macrophages, iNOS seemed to be involved in carcinogenesis and frequently expressed in tumor cells (4) and therefore potentially represents an exploitable target to enhance radio/chemosensitivity (9–11). Radiosensitization through iNOS could be induced by various cytokines (interferon [IFN]-γ, interleukin-1β), by toll-like receptor-4 agonists (lipopolysaccharide [LPS], lipid A, and OM-174), and by activated interferon-γ-secreting T cells (12–15). Oxygen consumption rates have not been examined in those experiments, and it remains unclear whether a respiratory response to NO contributed to the irreversible fixation of radiation-induced DNA damage, likely caused by both NO and oxygen (16, 17). Although inhibition of cellular respiration through NO has been documented (5), the radiobiologic consequence of this phenomenon has never, to our knowledge, been explored.

In this study, we examined whether activation of iNOS may counteract MOD and thereby improve radioresponse in a model of metabolic hypoxia. We assumed that iNOS may be expressed in both tumor cells and in macrophages, the major component of the tumor proinflammatory infiltrate (4, 18, 19). Classically, mouse macrophages can be activated by IFN-γ and LPS, and the induction of proinflammatory iNOS is often mirrored by heme oxygenase-1 (HO-1), a cytoprotective and antiinflammatory enzyme (20). As a result, carbon monoxide (CO) is released from heme, which might affect cellular respiration next to the effects of NO (21). On the basis of these considerations, we exposed mouse EMT-6 tumor cells and RAW 246.7 macrophages to LPS/IFN-γ and analyzed both types of cells for iNOS and HO-1. Next we examined tumor cells, either alone or combined with activated macrophages, for radiosensitivity and oxygen consumption.

METHODS AND MATERIALS

Chemicals

All chemicals were obtained from Sigma Chemical Co (St. Louis, MO), unless otherwise stated.

Cell culture

Murine mammary adenocarcinoma EMT-6 cells were kindly provided by Dr. Edith Lord (University of Rochester, Cancer Center, New York). Murine macrophage-like RAW 264.7 cells were obtained from European Collection of Cell Cultures (Wiltshire, UK). All experiments were performed in RPMI 1640 medium (Invitrogen) supplemented with 10% bovine calf serum (Greiner Bio-one, Belgium) in plastic flasks (Greiner, Frickenhausen, Germany).

Induction of iNOS and HO-1

The EMT-6 and RAW 264.7 cultures were grown to early confluence and exposed to LPS (0.1 μg/mL) plus IFN- γ (10 ng/mL) for 16 h. Alternatively, RAW 264.7 cultures were exposed to hemin (100 μM), a specific inducer of HO-I. Afterward, cells were collected by trypsinization and analyzed for oxygen consumption and radiosensitivity, as described later. The HO-1 inhibitor tin-protoporphyrin (SnPPIX) was used at 30 μM, and the iNOS inhibitor aminoguanidine (AG) was used at 1 mM and 3 mM for long-term (Griess assay) and short-term (MOD) treatments, respectively (14, 15).

Protein expression of iNOS and HO-1 by Western blotting

Cell lysates (from 2–10 $\times$ 10^5 cells) were subjected to electrophoresis in a 10% sodium dodecyl sulfate (SDS)-polyacrylamide gel, and the blots were processed for immunoperoxidase-based staining as previously described (14).

Gene expression of iNOS and HO-1 by reverse transcription polymerase chain reaction

Reverse transcription polymerase chain reaction (RT-PCR) was performed in an ABI PRISM 7000 sequence detection system. The target-specific unlabeled primers and Taqman minor groove binding probes (VIC dye labeled) for HO-1, iNOS, and 18S were supplied by Applied Biosystems as assays on demand. The relative expression (ΔC_T) of iNOS and HO-1 was normalized to the housekeeping 18S gene using the equation: ΔC_T = iNOS (or HO-1) C_T minus 18S C_T, where C_T is an arbitrary number of PCR cycles needed to pass threshold.

Enzymatic activity of iNOS and HO-1

The activity of iNOS was measured by the accumulation of nitrite, an oxidized metabolite of NO, in the medium using the Griess reaction (12). The activity of HO-1 was measured by the bilirubin generation from hemin, as described elsewhere (20, 21).

Oxygen consumption

Electron paramagnetic resonance oximetry was performed at a cell density of 10 $\times$ 10^6/mL with a spin probe ^{15}N 4-oxo-2, 2, 6, 6-tetramethylpiperidine-d16-1-oxyl (^{15}N PDT) at 0.2 mM, as previously described (6). Briefly, 100-μL aliquots of cells in 10% dextran in complete medium were drawn into glass capillary tubes, sealed, and placed into quartz EPR tubes at 37°C. The probe was calibrated so that the line width measurements could be related to the oxygen level. Oxygen consumption rates were expressed as the slope of the O_2 decline over time, which was generally linear within an oxygen range of 3–21%. At higher cell densities (30–50 $\times$ 10^6/mL), oxygen consumption was monitored by a Clark-type O_2 electrode in a gas-tight chamber under constant mixing.

Metabolic hypoxia and radiosensitization of EMT6 cells

Our principle model of hypoxia-induced radioresistance was based on a MOD at 10 $\times$ 10^6/mL to match the conditions of EPR

oximetry. Briefly, 300-μL aliquots of EMT-6 tumor cells were drawn into 1-mL syringes and sealed, and MOD was induced before radiation by a 15-min incubation at 37x°C under constant shaking. In mixed suspensions of tumor cells and macrophages, RAW 264.7 cells were lethally preirradiated at 100 Gy to avoid interference with the cell regrowth that had little if any effect on NO production. The reversal of hypoxic radioresistance through activation of iNOS (by LPS/IFN-γ) was examined either directly in iNOS-expressing tumor cells in the absence of macrophages or alternatively through a bystander mechanism in mixed suspensions of activated (NO-producing) macrophages and control tumor cell at a 1:1 ratio. Radiosensitization of EMT-6 tumor cells by RAW 264.7 macrophages at lower ratios (1:32–1:2) was performed in micropellets, an alternative model of metabolic hypoxia described in more detail previously (12–14). Briefly, 100-μL aliquots of 0.5×10^6/mL EMT-6 cells plus 0.5×10^6/mL preirradiated RAW 264.7 macrophages were placed in conical tubes and centrifuged for 5 min at 300*g* to produce the pellets. MOD was induced before radiation by a 5-min incubation at 37°C. Tumor cell survival after radiation (5, 10, and 15 Gy) was measured by an 8-day colony formation assay. A surviving fraction was calculated as a colony survival after radiation versus no radiation (0 Gy). Radiosensitization (enhancement ratio) was determined at a surviving fraction of 0.1. The plating efficiency of EMT-6 cells was 80–85% and was not affected by exposure to aminoguanidine during MOD induction.

Statistics

All assays were repeated at least three times. Data are expressed as mean with corresponding standard deviation. Western blots were taken from representative experiments.

RESULTS

Response of RAW 264.7 macrophages and EMT-6 tumor cells to LPS/IFN-γ

Both RAW 264.7 macrophages and EMT-6 tumor cells were exposed to a similar stimulation with LPS/IFN-γ, and the expression of iNOS and HO-1 was examined by RT-PCR, Western blotting, and enzymatic assays. In both tumor cells and macrophages, the iNOS RNA levels were upregulated until the ΔC_T values of 8–9 (versus 18S), consistent with a positive protein immunostaining (Fig. 1A and B). In addition, macrophages showed the activation of HO-1, which was confirmed for the alternative stimulation with hemin (Fig. 1D). The latter agent, as expected, was a specific activator of HO-1 only and did not induce iNOS (data not shown). In EMT-6 tumor cells, the iNOS profile generally matched that of macrophages, whereas HO-I was negative in both RT-PCR ($\Delta C_T > 11$) and Western blotting (Fig. 1C). Next, the activity profiles of both enzymes were examined and normalized to the same cell concentration of 10×10^6/mL, as in radiation and oxygen consumption experiments. Enzymatic activity of iNOS was determined by the nitrite production, an oxidative product of NO, whereas HO-1 was analyzed by the production of bilirubin that is released (next to CO) during the oxidative reaction of heme degradation. Stimulated RAW 264.7 and EMT-6 cells produced similar levels of nitrite (14 μM), which was completely blocked by aminoguanidine, which was further used in radiosensitizing experiments to dissect the effects of iNOS from HO-1 (Fig. 2A). The HO-1 activity ranged between 8 and 22 μM bilirubin,\ after stimulation with LPS/IFN-γ and hemin, respectively, and could be abolished by SnPPIX (Fig. 2B). This well-known HO-1 inhibitor, however, exerted considerable delayed toxicity and therefore was not used in radiation experiments. Instead, to dissect HO-1 from iNOS, we preferred to selectively induce HO-1 by hemin. To summarize in brief, LPS/IFN-γ induced a similar proinflammatory iNOS response in RAW 264.7 macrophages and EMT-6 tumor cells, whereas macrophages in addition featured coinduction of HO-1.

Radiosensitization of EMT-6 tumor cells through iNOS: direct and bystander effects

The previous set of data shows that macrophages and tumor cells may produce similar amounts of NO/nitrite upon exposure to LPS/IFN-γ. Therefore. we asked whether NO synthesized directly in tumor cells, or released from bystander macrophages, is an equally potent radiosensitizer. Radiosensitizing effects were analyzed in sealed cell suspensions, which consisted of 10×10^6/mL EMT-6 tumor cells, a standard cell density used in our EPR oximetry (6). At this cell concentration, the appearance of hypoxic radioresistance was already clearly detected at 15 min, as compared with aerobic cells (Fig. 3A). First, the radiosensitivity of EMT-6 tumor cells after exposure to LPS/IFN-γ was evaluated in the absence of macrophages. This direct treatment restored hypoxic radioresponse of tumor cells with an enhancement ratio of 2.3, hence resembling the aerobic radiosensitivity. Next, RAW 264.7 macrophages were activated by LPS/IFN-γ and mixed with control EMT-6 cells at a ratio of 1:1 (Fig. 3B). Bystander macrophages increased the radioresponse of tumor cells by 2.2-fold, thus closely approaching the direct radiosensitizing effect. The metabolic iNOS inhibitor aminoguanidine abolished the radiosensitizing effect of LPS/IFN-γ in both sets, thus implying the role of iNOS-mediated NO synthesis in radiosensitization. On the other hand, the HO-1–expressing macrophages (obtained by exposure to hemin) failed to radiosensitize tumor cells (Fig. 3B), further arguing against the role of HO-1 in hypoxic radioresponse. Considering these negative results, only iNOS (but not HO-1) was further explored as a determinant of cellular oxygen consumption.

Inhibition of oxygen consumption through iNOS

To link oxygenation and radioresponse, the oxygen consumption measurements were performed by EPR oximetry in the frame of radiosensitizing experiments. In sealed cell suspensions under matching metabolic conditions (10×10^6/mL at 37°C), the mean slopes for control EMT-6 tumor cells and RAW 264.7 macrophages (basal rates) were -1.59 and -0.77, respectively, suggesting that tumor cells consume oxygen significantly faster (Fig. 4A). Next, three graphs (Fig. 4B and D) demonstrate the inhibitory effect of iNOS on respiration, and each pair of slopes shows the switch from NO production to NO block by aminoguanidine. Indeed, in NO-producing EMT-6 and RAW 264.7 cells

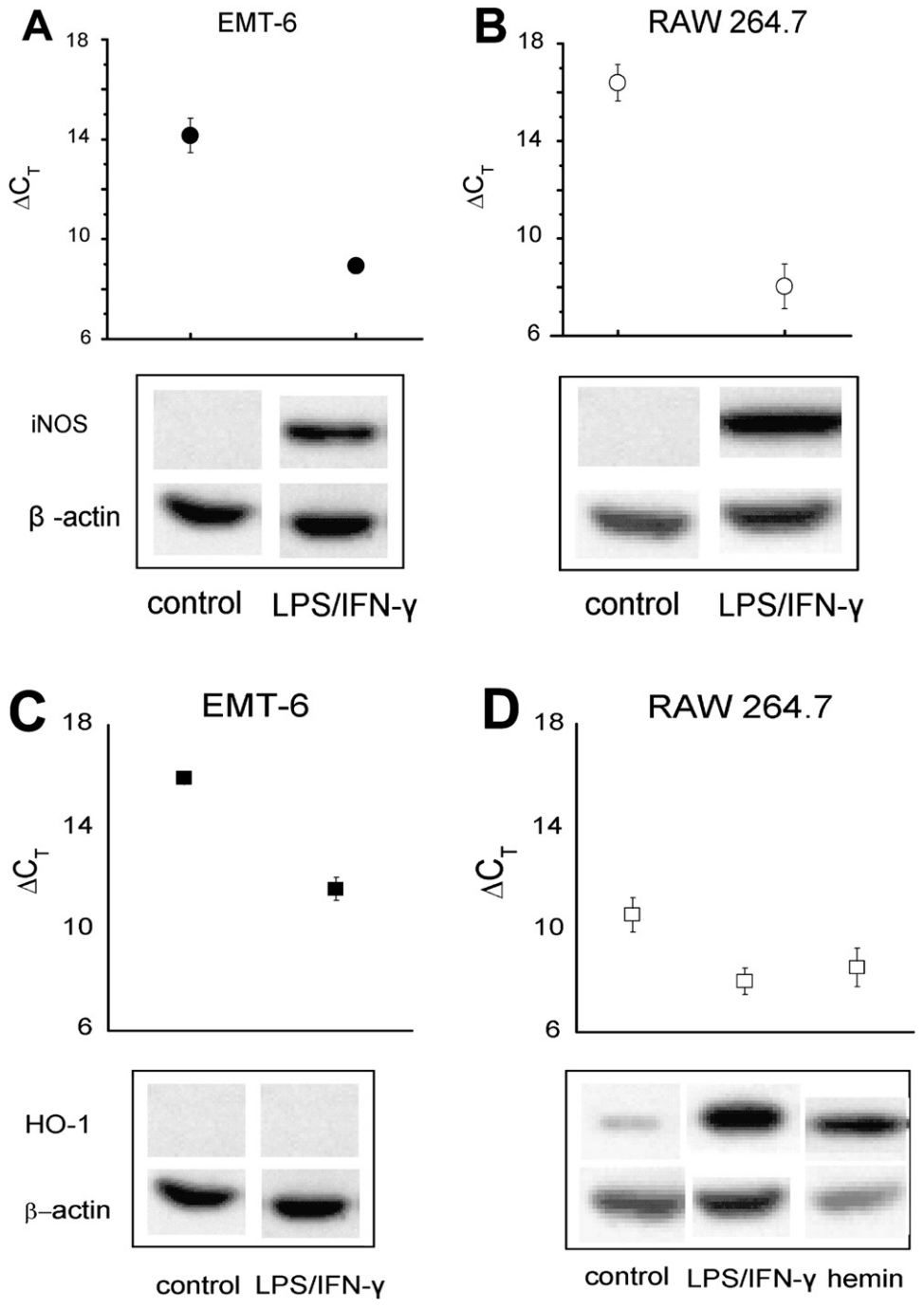

Fig. 1. Activation of inducible nitric oxide synthase (iNOS) and heme oxgenase-1 (HO-1) in EMT-6 tumor cells and RAW 264.7 macrophages, as analyzed by reverse transcription polymerase chain reaction (RT-PCR) and Western blotting. EMT-6 tumor cells (A and C) and RAW 264.7 macrophages (B and D) were exposed to lipopolysaccharide (LPS) plus interferon (IFN)-γ (0.1 μg/mL plus 10 ng/mL) or hemin (100 μM) for 16 h and examined for iNOS (A and B) and HO-1 (C and D). Relative gene expression (ΔC_T) was normalized to 18S, and relative protein expression was validated by β-actin. The RT-PCR data are the mean of four repeats; Western blotting was chosen from three representative experiments.

(apart), aminoguanidine restored the oxygen consumption rates from −0.64 to −1.66 and from −0.27 to −0.65, thus by 2.5 and 2.4-fold, respectively (Fig. 4B and C). Next, we verified whether NO-producing macrophages can inhibit oxygen consumption in mixed cell suspensions with control tumor cells at a ratio of 1:1 (Fig. 4D). Under aminoguanidine block, we observed a 1.9-fold increase in oxygen consumption (from 0.80 to −1.49), an effect that is most likely dependent on tumor cells because macrophages, activated or not, were consuming 2.1-fold less oxygen. This means that NO produced in activated macrophages may easy diffuse to adjacent tumor cells and thereby counteract oxygen consumption through a bystander effect. All the above EPR measurements are summarized in Fig. 4E, where data are expressed as paired slope

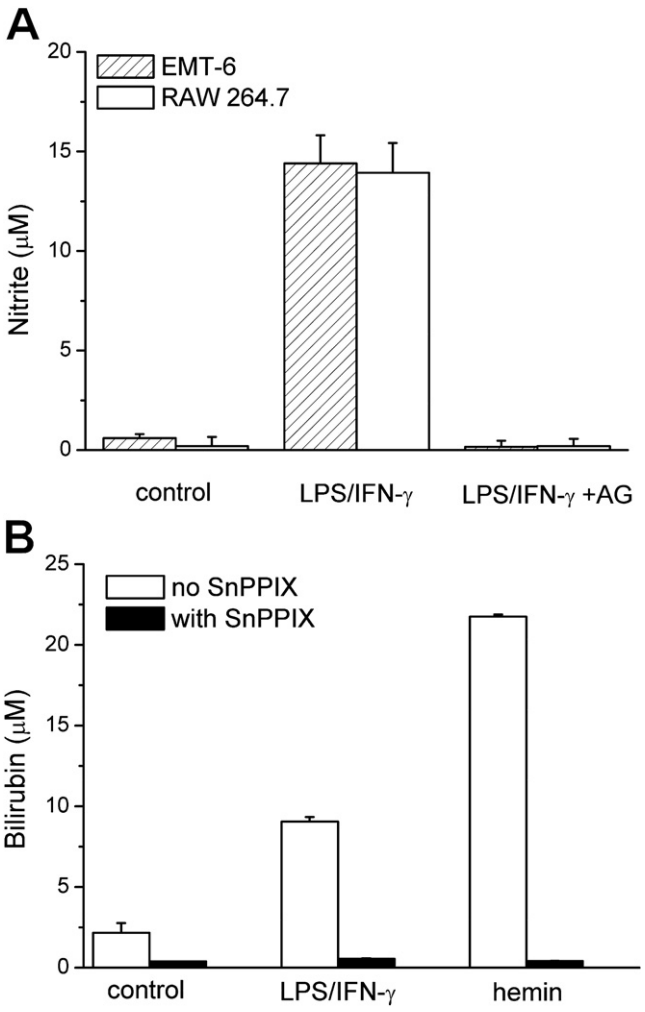

Fig. 2. Enzymatic activity of inducible nitric oxide synthase (iNOS) and heme oxgenase-1 (HO-1) in EMT-6 and RAW 264.7 cells. (A) EMT-6 and RAW 264.7 cells were exposed to lipopolysaccharide (LPS) plus interferon (IFN)-γ (0.1 μg/mL plus 10 ng/mL) or hemin (100 μM) for 16 h. (A) Cell suspensions (10×10^6/mL) were incubated for 30 min, and supernatants were analyzed for nitrite, a marker of iNOS activity. (B) Microsomal fractions of RAW 264.7 cells (10×10^6 mL) were analyzed for bilirubin, a marker of HO-1 activity. To inhibit iNOS and HO-1, aminoguanidine (AG) and tin-protoporphyrin (SnPPIX) were used at 3 mM and 30 μM, respectively. Data are the mean of four repeats.

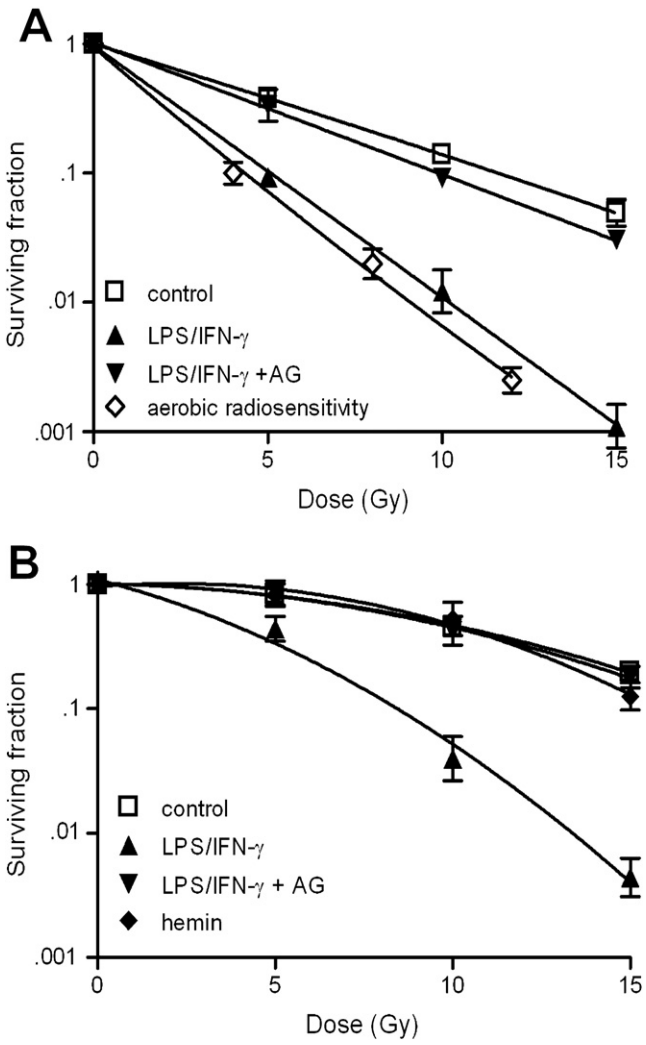

Fig. 3. Radiosensitization of EMT-6 tumor cells through inducible nitric oxide synthase (iNOS). (A) EMT-6 cells were exposed to lipopolysaccharide (LPS) plus interferon (IFN)-γ (0.1 μg/mL plus 10 ng/mL) for 16 h. The aerobic radiosensitivity was provided for reference to scale hypoxia-induced radioresistance. (B) RAW 264.7 macrophages were exposed to LPS/IFN-γ or hemin (100 μM) for 16 h and mixed with control EMT-6 tumor cells at a ratio of 1:1. To inhibit iNOS, aminoguanidine (AG) was used at 3 mM. Data are the mean of four repeats.

coefficients, and further confirmed by a Clark-type at higher cell densities of 30–50 $\times$ 10^6/mL (Fig. 4F). In control EMT-6 cells, oxygen was progressively consumed, leading to a deep hypoxia below 1% oxygen, whereas iNOS activation by LPS/IFN-γ resulted in a profound sparing of oxygen over 5%. Inasmuch as radiosensitizing experiments and oxygen measurements were performed in the same model of metabolic hypoxia, we conclude that iNOS induction, either directly in EMT-6 tumor cells or in bystander RAW 264.7 macrophages, is the crucial mechanism of oxygen sparing and overcoming hypoxic radioresistance. This mechanism can be abolished through the metabolic block of iNOS by aminoguanidine, which in parallel counteracts NO/nitrite production, oxygen sparing, and eventually radiosensitization.

Radiosensitizing potential of activated macrophages

To further clarify the radiosensitizing potential of bystander macrophages, we next examined the limits of macrophage-to-tumor cells ratios that are sufficient to radiosensitize tumor cells. Inasmuch as the local level of NO production should be proportional to a cell concentration, we have used another model of metabolic hypoxia, namely micropellets (cell density approximately 300 x 10^6/ml), which contained the fixed amount of EMT-6 tumor cells (0.5 x 10^6) and RAW 264.7 macrophages added at a ratio from 1:32 to 1:2. This model mimicked a diffusion-limited oxygenation leading to hypoxia-induced radioresistance, inasmuch as the surviving fraction of control EMT-6 cells, both alone or mixed with control macrophages, was between

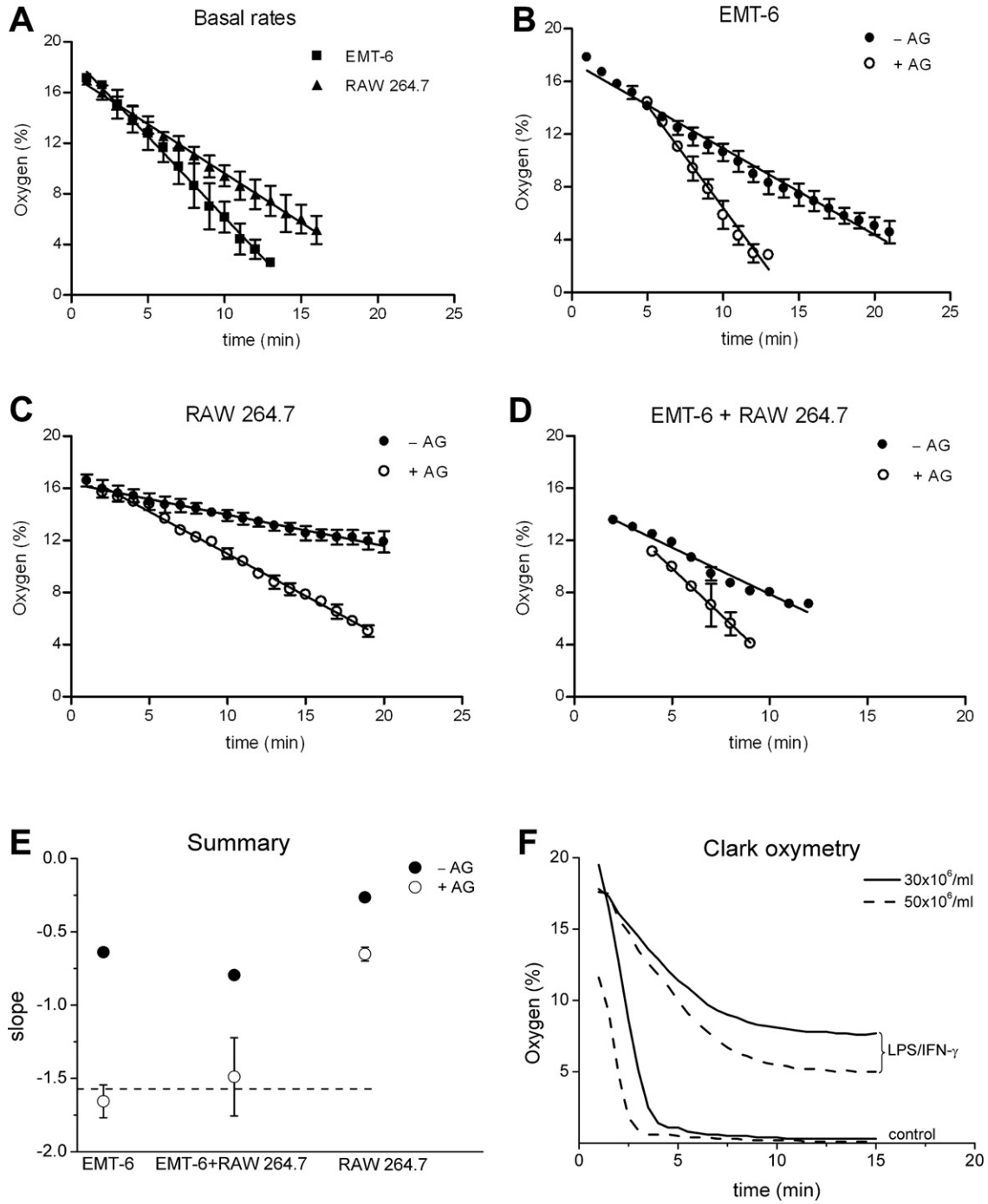

Fig. 4. Inhibition of oxygen consumption by inducible nitric oxide synthase (iNOS). EMT-6 and RAW 264.7 cells were treated with lipopolysaccharide (LPS) plus interferon (IFN)-γ (0.1 μg/mL plus 10 ng/mL) for 16 h. Oxygen levels were measured either by EPR oxymetry (A–E) or by a Clark-type electrode (F). (A) Basal oxygen consumption rates in control EMT-6 and RAW 264.7 cells. (B, C, and D) The switch of oxygen consumption by the iNOS inhibitor aminoguanidine (AG) in NO-producing EMT-6 (B), RAW 264.7 (C), and mixed (1:1) RAW 264.7/EMT-6 cells (D). In the last set (D), only RAW 264.7 cells were exposed to LPS/IFN-γ and AG, and mixed with control EMT-6 cells. (E) Summary of A–D, expressed as the slope coefficients, which were referred to the basal rate of oxygen consumption in control EMT-6 cells (interrupted line). (F) Induction of deep hypoxia (below 1% oxygen) in control EMT-6 cells, as opposed to oxygen sparing through iNOS induction. To inhibit iNOS, AG was used at 3 mM. Data are the mean of four repeats; the last set (F) is a representative measurement.

0.1-0.3 at 10 Gy (Fig. 5). Note that aerobic cell survival at this dose of radiation was below 0.01 (Fig. 3A). Activation of macrophages by LPS/IFN-γ resulted in an efficient radiosensitization of EMT-6 cells at ratios above 1:16. This bystander effect was comparable with direct activity found in iNOS-expressing EMT-6 cells alone, in line with experiments performed in sealed cell suspensions (Fig. 3A and B). Once again, HO-1–expressing macrophages, obtained

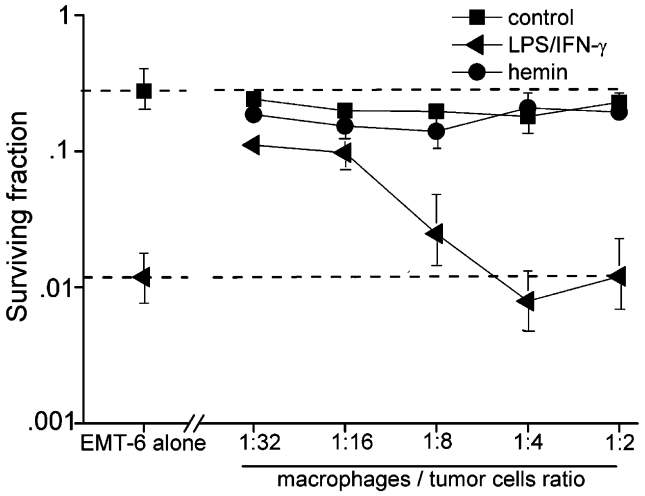

Fig. 5. Radiosensitization of EMT-6 tumor cells by activated RAW 264.7 macrophages. Hypoxic radiosensitivity was accessed in a micropellet model using specified ratios of macrophages and tumor cells. RAW 264.7 macrophages were exposed to lipopolysaccharide (LPS) plus interferon (IFN)-γ (0.1 μg/mL plus 10 ng/mL) or hemin (100 μM) for 16 h and mixed with control EMT-6 tumor cells. Direct radiosensitization of EMT-6 tumor cells by LPS/IFN-γ is provided for reference (interrupted line). Data are the mean of three repeats.

by exposure to hemin, failed to radiosensitize tumor cells. This confirms, that the principal mechanism by which activated RAW 264.7 macrophages radiosensitize EMT-6 tumor cells is not linked to HO-1 but is associated with the iNOS/NO pathway.

DISCUSSION

The principal finding of our study is that inhibition of cellular respiration through the iNOS/NO pathway may efficiently counteract MOD and hypoxia-induced radioresistance in tumor cells. This has been confirmed in both isolated tumor cells and in tumor cells combined with macrophages at different ratios, modeling the tumor microenvironment with regard to the proinflammatory infiltrate. Four conclusions can be drawn from oxygen consumption measurements performed either by EPR or a clark-type oximetry. First, the induction of iNOS resulted in a 2- to 3-fold decline in the initial slopes of oxygen consumption in both EMT-6 tumor cells and RAW 264.7 macrophages. Tumor cells consumed up to 2.1 times more oxygen than macrophages, suggesting that they were primarily responsible for MOD in mixed cell suspensions. Second, aminoguanidine, a metabolic inhibitor of iNOS-mediated NO synthesis, reversed MOD in both types of cells and in mixed cell suspensions, thus providing a selective tool to affect MOD-dependent radioresistance. Third, the bystander effect of activated NO-producing macrophages closely approached the direct effect of NO endogenously produced inside tumor cells. This can be explained by the remarkable diffusion properties of NO, which is not metabolically consumed in contrast to oxygen. Finally, the induction of radiobiologically relevant hypoxia (below 1% oxygen) could be revealed in iNOS-silent tumor cells only, whereas iNOS activation efficiently reversed MOD with an oxygen-sparing effect above 5%. Collectively, these findings provide evidence that the iNOS and oxygen consumption profiles are inversely linked and that activation of macrophages may favor oxygen sparing in tumor cells. It remains to clarify whether NO effects are more pronounced in tumor cell types that reveal high respiratory rates.

Over the past decade, the multifaceted role of NO in cancer biology had been strongly emphasized (4, 10). It has been suggested that low basal levels of NO may be carcinogenic and angiogenic, thus promoting the growth of primary tumors and metastases. By contrast, optimal iNOS activation was shown to induce apoptosis and to exert antitumor and antimetastatic effects. Besides, at micromolar concentrations, both NO and its oxidative product nitrite are known to downregulate respiratory mitochondrial functions, in a variety of cells including tumor cells, macrophages, astrocytes, hepatocytes and myocytes (5, 10, 22). The observed levels of NO/nitrite production in both EMT-6 tumor cells and RAW 264.7 macrophages after exposure to LPS/IFN-γ matched those concentrations. Indeed, we found up to 14 μM nitrite at used cell densities (10×10^6/mL), consistent with a high iNOS expression in Western blotting and RT-PCR. In activated macrophages (but not in EMT-6 cells), we also detected the upregulation of the inducible heme oxygenase-1 (HO-1), which is often co-induced in macrophages and seems to defend them from NO cytotoxicity by releasing the protective molecule CO (and bilirubin) from heme (20, 21). The radiosensitizing potential of bystander NO and CO-producing macrophages was further examined in two models of metabolic hypoxia in comparison with direct NO effects in iNOS-expressing tumor cells.

We observed a 2.4 times radioprotection of hypoxic iNOS-silent EMT-6 cells compared with aerobic counterparts, thus approaching a classic radioresistance in chronic hypoxia in a nitrogen-based atmosphere (15). In line with MOD inhibition, NO-producing tumor cells showed restored radiosensitivity, whereas iNOS inhibition by aminoguanidine abolished both respiratory and radiation effects. The same pattern of radiosensitizing effects could be induced by bystander NO-producing macrophages, whereas CO-producing macrophages failed to show any radiomodulation. We cannot rule out that our acute metabolic model is not optimal to uncover the effect of CO on mitochondrial respiration, recently described by D'Amico *et al*. (21). Indeed, CO was shown to exclusively target the reduced form of cytochrome c oxidase obtained by a prolonged cell pre-incubation in 1% oxygen. By contrast, NO could interact with both reduced and oxidized enzymes, and it profoundly blocked cellular respiration. Our data were consistent with the last observation and projected the importance of NO to control both respiration and radioresponse in tumor cells. In summary, our studies now suggest four possible mechanisms by which NO may improve tumor cell radioresponse: (*1*) enhanced DNA damage by analogy to the direct fixation effects of oxygen (16, 17); (*2*) increased oxygenation through eNOS-mediated

vasodilation or oxygen sparing (6, 7); (*3*) direct MOD block in iNOS-expressing tumor cells; and (*4*) indirect MOD block by NO-producing macrophages through a bystander effect.

It is well accepted that classic M1 polarization of macrophages is an important prerequisite for Th1 polarization in adaptive T-cell immunity driven by IL-12 and IFN-γ and that tumor hypoxia may inhibit this polarization (18, 19, 23). We have previously documented both IL-12 and IFN-γ as potent radiosensitizers (14) and have demonstrated the radiosensitizing ability of activated CD8 + T cells through the secretion of IFN-γ (15). Those effects, however, could be revealed in iNOS-expressing tumor cells only, because radiosensitization was caused by NO produced inside tumor cells. The current study represents the next step in our radiosensitizing strategy, designed to engage iNOS-silent tumor cells as well. Our data now provide evidence that activated macrophages are able to counteract MOD and hypoxic radioresistance in tumor cells through a bystander effect of NO. In a physiologic model of metabolic hypoxia, clear radiosensitizing effects could be achieved at ratios ranging between 1:16 to 1:1, which are relevant for the majority of solid tumors.

CONCLUSION

Collectively, our findings illuminate NO-producing macrophages as a novel determinant of tumor cell radioresponse. In addition, tumor-associated macrophages, an important focus in tumor immunology and an attractive target in immunostimulatory strategies, may become a mechanistic link between immunotherapy and radiotherapy.

REFERENCES

1. Brown JM, Wilson WR. Exploiting tumour hypoxia in cancer treatment. *Nat Rev Cancer* 2004;4:437–447.
2. Dewhirst MW, Navia IC, Brizel DM, *et al*. Multiple etiologies of tumor hypoxia require multifaceted solutions. *Clin Cancer Res* 2007;13:375–377.
3. Crokart N, Jordan BF, Baudelet C, *et al*. Glucocorticoids modulate tumor radiation response through a decrease in tumor oxygen consumption. *Clin Cancer Res* 2007;13:630–635.
4. Wink DA, Vodovotz Y, Laval J, *et al*. The multifaceted roles of nitric oxide in cancer. *Carcinogenesis* 1998;19:711–721.
5. Brown GC. Nitric oxide and mitochondrial respiration. *Biochim Biophys Acta* 1999;1411:351–369.
6. Jordan BF, Gregoire V, Demeure RJ, *et al*. Insulin increases the sensitivity of tumors to irradiation: Involvement of an increase in tumor oxygenation mediated by a nitric oxide-dependent decrease of the tumor cells oxygen consumption. *Cancer Res* 2002;62:3555–3561.
7. Jordan BF, Sonveaux P, Feron O, *et al*. Nitric oxide as a radiosensitizer: Evidence for an intrinsic role in addition to its effect on oxygen delivery and consumption. *Int J Cancer* 2004;109:768–773.
8. Janssens MY, Van den Berge DL, Verovski VN, *et al*. Activation of inducible nitric oxide synthase results in nitric oxide-mediated radiosensitization of hypoxic EMT-6 tumor cells. *Cancer Res* 1998;58:5646–5648.
9. De Ridder M, Verellen D, Verovski VN, *et al*. Hypoxia tumor cell radiosensitization through nitric oxide. *Nitric Oxide* 2008;19:164–169.
10. Sonveaux P, Jordan BF, Gallez B, *et al*. Nitric oxide delivery to cancer: Why and how? *Eur J Cancer* 2009;45:1352–1369.
11. Fitzpatrick B, Mehibel M, Cowen RL, *et al*. iNOS as a therapeutic target for treatment of human tumors. *Nitric Oxide* 2008;19:217–224.
12. De Ridder M, Van den Berge DL, Verovski VN, *et al*. NF-kappaB inhibition impairs the radioresponse of hypoxic EMT-6 tumour cells through downregulation of inducible nitric oxide synthase. *Br J Cancer* 2003;88:120–124.
13. De Ridder M, Verovski VN, Van den Berge DL, *et al*. Lipid a radiosensitizes hypoxic EMT-6 tumor cells: role of the NF-kappaB signaling pathway. *Int J Radiat Oncol Biol Phys* 2003;57:779–786.
14. De Ridder M, Verovski VN, Chiavaroli C, *et al*. The radiosensitizing effect of immunoadjuvant OM-174 requires cooperation between immune and tumor cells through interferon-gamma and inducible nitric oxide synthase. *Int J Radiat Oncol Biol Phys* 2006;66:1473–1480.
15. De Ridder M, Jiang H, Van Esch G, *et al*. IFN-gamma+ CD8 + T lymphocytes: possible link between immune and radiation responses in tumor-relevant hypoxia. *Int J Radiat Oncol Biol Phys* 2008;71:647–651.
16. Mitchell JB, Wink DA, DeGraff W, *et al*. Hypoxic mammalian cell radiosensitization by nitric oxide. *Cancer Res* 1993;53:5845–5848.
17. Verovski VN, Van den Berge DL, Soete GA, *et al*. Intrinsic radiosensitivity of human pancreatic tumour cells and the radiosensitising potency of the nitric oxide donor sodium nitroprusside. *Br J Cancer* 1996;74:1734–1742.
18. Sica A, Larghi P, Mancino A, *et al*. Macrophage polarization in tumour progression. *Semin Cancer Biol* 2008;18:349–355.
19. Weigert A, Brune B. Nitric oxide, apoptosis and macrophage polarization during tumor progression. *Nitric Oxide* 2008;19:95–102.
20. Srisook K, Cha YN. Biphasic induction of heme oxygenase-1 expression in macrophages stimulated with lipopolysaccharide. *Biochem Pharmacol* 2004;68:1709–1720.
21. D'Amico G, Lam F, Hagen T, *et al*. Inhibition of cellular respiration by endogenously produced carbon monoxide. *J Cell Sci* 2006;119:2291–2298.
22. Frerart F, Sonveaux P, Rath G, *et al*. The acidic tumor microenvironment promotes the reconversion of nitrite into nitric oxide: Towards a new and safe radiosensitizing strategy. *Clin Cancer Res* 2008;14:2768–2774.
23. Lewis CE, Pollard JW. Distinct role of macrophages in different tumor microenvironments. *Cancer Res* 2006;66:605–612.